THE EFFECT OF EVOLVING GAS DISTRIBUTION ON SHALLOW LUNAR MAGMATIC INTRUSION DENSITY: IMPLICATIONS FOR GRAVITY ANOMALIES. L. M. Jozwiak[1], J. W. Head[1], G. A. Neumann[2], L. Wilson[3], [1]Dept. Earth, Environmental and Planetary Sciences, Brown University, Providence, RI 02906. [2]Solar System Exploration Div., NASA Goddard Space Flight Center, Greenbelt, MD 20768. [3]Lancaster Environment Centre, Lancaster University, Lancaster LA1 4YQ, UK. (lauren_jozwiak@brown.edu)

Introduction: The GRAIL (Gravity Recovery and Interior Laboratory [1]) mission has enabled unprecedented views of the lunar crust and interior structure. Indeed, the data solutions now resolve gravity anomalies arising from lateral heterogeneities within the crust globally at scales < 10 km[2,3]. Intrusive magmatic features such as dikes and sills are predicted to be prevalent within the lunar crust [4] and gravity data present a unique way of investigating their presence. Recently, GRAIL data were used to interpret the presence of large, ancient dikes within the lunar crust [5]; however, as yet, the detection of smaller scale dikes and sills has proven difficult due to their moderate spatial dimensions and uncertain density contrast.

Recent morphologic studies [6, 7] have supported the hypothesis that members of the class of lunar craters known as floor-fractured craters (FFCs) were formed by the intrusion and evolution of a shallow magmatic body beneath the crater. The presence of a large magmatic intrusion beneath these craters should be easily visible in the observed crater Bouguer gravity anomaly.

Using the FFC Alphonsus as an example, we examine the observed Bouguer anomaly and compare this to idealized predictions of the Bouguer anomaly, which are based on predicted intrusion thickness from crater morphology [6, 7]. We also examine processes within the magmatic intrusion which could alter the intrusion density, and hence affect the Bouguer anomaly. Specifically, we examine how volatiles within the intrusion and intrusion degassing affect the overall intrusion density.

Comparison of Predicted and Observed Gravity Signature: The crater Alphonsus, D = 119 km, (13.4°S, 2.8°W) is a class 5 FFC [6], possessing a flat floor profile and numerous dark-halo craters [8] identified as pyroclastic deposits [9] located along the crater floor fractures (Fig. 1a).

Using LOLA (Lunar Orbiter Laser Altimeter) data, we measure the crater depth as ~2.7 km, compared with 4.4 km depth suggested by the empirically derived crater depth v. diameter relationships developed by Pike (1980) [10]. We thus infer a maximum intrusion thickness of 1.69 km, ~1.7 km, beneath the crater [6]. We assume a lunar magma density of 3000 kg/m^3 [11] and a lunar crustal density of 2550 kg/m^3 [12]. Assuming the sill morphology can be modeled approximately as a Bouguer plate, an intrusion of constant thickness and large extent will generate a positive Bouguer anomaly of ~30 mGal.

Figure 1b shows the band-filtered Bouguer anomaly for the crater Alphonsus, filtered between orders 100-600. The data were generated using the GRGM900c spherical harmonic solution [2], and band-filtered to strongly attenuate anomaly contributions from regions deeper than ~34 km. The most prominent feature is the broad positive anomaly region in the northeastern quadrant of the crater floor, which has a magnitude of ~15 mGal, peaking in places at 30 mGal. The remaining crater floor area has a positive anomaly of magnitude 5-10 mGal. We note the spatial correlation between the large, broad positive anomaly in the NE quadrant and the location of a large number of dark-halo craters and fractures (compare Figure 1a and Figure 1b). Overall, the observed anomaly magnitude within the crater floor region is difficult to distinguish from that in the surrounding region, and is smaller than the magnitude of anomaly predicted from the intrusion morphology.

Given the numerous surficial volcanic features and morphologic evidence supporting the existence of a large magmatic body beneath Alphonsus, we now examine processes inherent to the evolution of magmatic intrusions, which could potentially alter the intrusion density.

Volatile Fraction and Degassing of Magmatic Intrusions: During the formation and evolution of the magmatic intrusion, there are numerous processes which occur, summarized schematically in Figure 2. One of the most important processes is the formation of a magmatic foam at the tip of the dike [13] and corresponding top of the intrusion. The existence of numerous pyroclastic deposits on the floor of Alphonsus [9] provides evidence for volatile build up and explosive venting of the magma. Using the method outlined by Head et al. (2002) [13] and Wilson et al. (2014) [14], and the process described in Wilson and Head (2003) [15] we can infer the volatile mass fraction released during the formation of the pyroclastic deposit. The average velocity of the pyroclasts can be calculated using the radius of the dark halo deposit, R [13, 14]:

$$R = v^2/g \quad (1)$$

Given the average dark halo radius of 3-4 km [8], the inferred eruption velocity is 70-80 m/s. This can be used to calculate the magmatic volatile gas fraction, n, from

$$n = [(v^2\, m\, (\gamma - 1)/(2\, Q\, T\, \gamma)]^{1/2} \quad (2)$$

which is a compromise between adiabatic gas expansion and gas expansion in the Knudsen regime [14]. Here m is the gas molecular weight, 28 kg kmol^{-1}, Q is the

universal gas constant, 8314 J $K^{-1}kmol^{-1}$, T is the magmatic temperature, 1500 K, γ is the ratio of gas specific heats, 1.28 (a weighted average of CO and H_2O, the two most common volatile species). We note that CO is the most common volatile species and is produced by oxidation-reduction reactions between graphite and metal oxides at pressures less than ~40 MPa [16], and H_2O is commonly released during exsolution of lunar magmas [17]. For the observed pyroclast ranges, this suggests a gas fraction of 0.0345, i.e. 3.45 mass %. Inverting the method of [14], and using the calculated pyroclast gas fraction, we determine a gas volume fraction of 72.8% within the foam, and a corresponding magma volume fraction of 27.2%. This gas volume fraction is near the theoretical limit of 80% [18] suggesting efficient volatile degassing, consistent with rapid foam formation during the initial formation of the sill. The density of CO gas at intrusion temperatures and pressures is 40 kg/m^3 and magma density is 3000 kg/m^3 [14]. Combined with the gas volume fractions, this equates to a foam layer density of 845 kg/m^3 ((40*0.728)+(3000*0.272)).

It is currently unknown how much of the intrusion volume will be occupied by this magmatic foam, although we are currently working on methods for calculating it. Thus, we present two possible scenarios: 1) foam layer equivalent to 25% of the intrusion volume, and 2) foam layer equivalent to 5% of the intrusion volume. For the conditions of scenario 1, the total intrusion density would be 2461 kg/m^3, which is slightly lower than the average lunar crustal density of 2550 kg/m^3. For the conditions of scenario 2, the total intrusion density would be 2892 kg/m^3, which is closer to, but still below, the commonly assumed fully degassed intrusion density.

Implications for Gravity Anomalies: We have shown that the inclusion of a volatile rich magmatic foam at the top of shallow magmatic intrusions on the Moon has a significant effect on the overall intrusion density. This change in density will significantly alter the observed Bouguer anomaly. For the crater Alphonsus, this process can help explain the difference in predicted Bouguer anomaly (based on a completely degassed intrusion) and the observed Bouguer anomaly (Figure 1b). We also suggest that during intrusion evolution, both passive degassing (such as along fractures) and active degassing (such as pyroclastic deposit formation) can alter the local foam thickness beneath the crater floor, leading to the heterogeneous Bouguer anomalies and the apparent correlation of more positive Bouguer anomalies with surficial volcanic deposits.

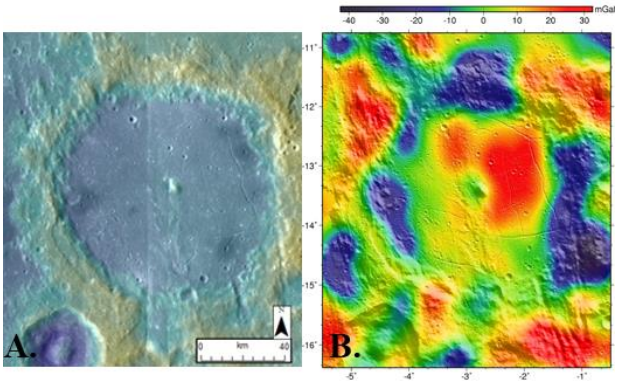

Figure 1: Floor-fractured crater Alphonsus, D = 119 km, (13.4°S, 2.8°W). **A)** The most prominent features of Alphonsus are the dark-halo craters which lie along the numerous floor fractures. **B)** Band-filtered Bouguer gravity anomaly for the crater Alphonsus, with emphasis drawn to the large positive anomaly region in the NE crater floor quadrant. LOLA topography data (color-coded blue-low, red-high) overlain by LROC-WAC image data (**A**). GRGM 900c Bouguer gravity solution band-filtered between orders 100-600 (**B**).

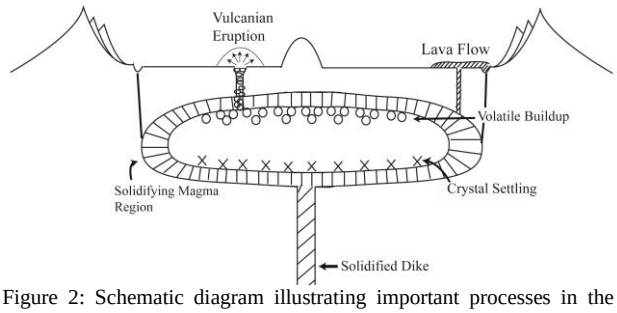

Figure 2: Schematic diagram illustrating important processes in the physical, thermal and temporal evolution of the floor-fractured crater magmatic intrusions. We specifically focus on the volatile build-up at the top of the intrusion and the relationship of this process to vulcanian eruptions which lead to the production of the dark halo craters.

References: [1] Zuber, M. T., et al. (2013) *Science, 339,* 668-671. [2] Lemoine, F.G., et al. (2013) *JGR 118*, 1676-1698. [3] Konopliv, A.S., et al. (2013) *JGR 118*, 1415-1434. [4] Head, J. W. and Wilson, L. (1992) *Geochim. et. Cosmochim. Acta, 56,* 2155-2175. [5] Andrews-Hanna, J. C., et al. (2013) *Science, 339,* 675-678. [6] Jozwiak, L. M., et al. (2012) *JGR, 117*, E11. [7] Jozwiak, L. M., et al. (2015) *Icarus, 248,* 424-447. [8] Head, J. W. and Wilson, L. (1979) *Proc. Lunar Planet. Sci. Conf. 10th*, 2861-2897. [9] Gaddis, L. R., et al. (2003) *Icarus, 161*, 262-280. [10] Pike, R. J. (1980) *USGS Prof. Paper 1046-C*. C1-C77. [11] Kiefer, W. S., et al. (2012) *GRL, 39*, L07201. [12] Wieczorek, M. A., et al. (2013) *Science, 339*, 671-675. [13] Head, J. W., et al. (2002) *JGR, 107*, E1, 5001. [14] Wilson, L., et al. (2014) *LPSC XLV*, Abstract #1223. [15] Wilson, L. and Head, J.W. (2003) *GRL 30*, 1605. [16] Rutherford, M. and Papale, P. (2009) *Geology, 37*, 219-222. [17] Saal, A. E., et al. (2008) *Nature, 454*, 192-196. [18] Jaupart, C. and Vergniolle, S. (1989) *J. Fluid Mech., 203*, 347-380.